



## Oxacyanopyridine-Benzofuran Hybrids: Synthesis, *in silico* Toxicity Assessment, *in vitro* Antimicrobial Activity and Dual Target Docking Studies

BHARGAVI POSINASETTY<sup>1</sup>, ASHISH ASHOKKUMAR JAISWAL<sup>2</sup>, RAJENDRA PRASAD YEJELLA<sup>3</sup>,  
HARI VELURU<sup>4</sup>, KISHORE BANDARAPALLE<sup>5</sup> and RAJASEKHAR KOMARLA KUMARACHARI<sup>6,\*</sup>

<sup>1</sup>Department of Dentistry, Government Dental College and Research Institute, Bellary-583104, India

<sup>2</sup>HKE Society's Matoshree Taradevi Rampure Institute of Pharmaceutical Sciences, Kalaburagi-585105, India

<sup>3</sup>Department of Pharmaceutical Chemistry, University College of Pharmaceutical Sciences, Andhra University, Visakhapatnam-530003, India

<sup>4</sup>Department of Pharmacology, MB School of Pharmaceutical Sciences, Mohan Babu University, Sree Sainath Nagar, A Rangampet, Tirupati-517102, India

<sup>5</sup>Department of Pharmaceutics, Sri Padmavathi School of Pharmacy, Tiruchanur, Tirupati-517503, India

<sup>6</sup>Department of Pharmaceutical Chemistry, Sri Padmavathi School of Pharmacy, Tiruchanur, Tirupati-517503, India

\*Corresponding author: Fax: +91 877 2237732; E-mail: komarla.research@gmail.com

Received: 12 December 2023;

Accepted: 15 January 2024;

Published online: 28 February 2024;

AJC-21549

This study emphasizes the synthesis and characterization of a novel series of oxa cyano pyridine heterocyclic molecular hybrids (**OCP 1-6**), integrating pyridine and benzofuran motifs. Meticulously designed from 5-chlorosalicylaldehyde in a multistep process, the synthesized compounds were structurally confirmed through IR spectroscopy, <sup>1</sup>H NMR spectroscopy, and mass spectrometry. Computational predictions highlighted diverse properties, including antitubercular and antibacterial attributes, bioactivity scores, toxicity profiles and potential molecular targets. *In vitro* assessments and Schrödinger docking simulations revealed binding affinities to enzymes viz. *Mycobacterium tuberculosis* enoyl-ACP reductase and *Escherichia coli* Topoisomerase IV. Compounds, particularly **OCP 2, 3, 4** and **5**, exhibited significant antitubercular and antibacterial activities in both *in vitro* assessments and docking simulations. This study underscores the substantial potential of the synthesized hybrids as promising candidates for further lead optimization, positioning them as valuable contributors to the development of pharmaceutical agents with heightened potency and enhanced safety profiles.

**Keywords:** Oxacyano pyridine, Benzofuran, Antitubercular activity, Antibacterial activity, Dual target docking.

### INTRODUCTION

Heterocyclic molecular hybrids, formed by merging distinct heterocyclic rings, are pivotal in medicinal chemistry, designed to optimize drug properties [1,2]. Pyridines and benzofurans, representing unique heterocyclic compounds, exhibit diverse structural and biological properties [3]. Pyridine is ubiquitously found as a six-membered heteroaromatic nucleus in several natural sources, such as alkaloids and vitamins. Recognized for its pharmacophoric potential, pyridine derivatives showcase antibacterial [4], antitubercular [5], antifungal [6], anticancer [7], anti-inflammatory [8], antimicrobial and antiviral [9] properties. Notably, pyridine compounds with a cyano-substituent at position-3 have shown promising applications in treating various diseases [10].

Benzofurans, with a fused benzene ring and an oxygen atom in a five-membered ring, are essential in organic synthesis, known for their diverse properties, including antitubercular [11], antibacterial [12], antifungal [13], anti-inflammatory [14], antimicrobial, anticancer, antioxidant and anti-Alzheimer's effects [15]. The fusion of pyridines and benzofurans into hybrids represents an exciting frontier in medicinal chemistry and drug discovery [16]. By combining these elements, researchers can design molecules with enhanced bioactivity, improved pharmacokinetics and a broader therapeutic application range [17-19].

Expanding on previous investigations into heterocyclic small molecules, and drawing inspiration from studies involving pyridine and benzofuran derivatives [20-22], our research achieves a significant milestone with the successful synthesis of pyridine-benzofuran hybrids. This synthesis embodies a meti-

culous design targeting specific pharmacophores, reflecting a strategic approach in the pursuit of novel compounds with enhanced therapeutic properties. Focusing on the global challenges of infectious diseases and antibiotic resistance [23-25], present study is dedicated to unraveling the inherent antimicrobial properties of these hybrids. With the potential to contribute substantially to effective solutions against infectious diseases, the synthesized compounds mark a pivotal step forward in medical therapeutics.

To understand these synthesized molecules, the computational tools, including PASS, Syntelly and PLATO as well as the dual-target docking studies [26] were introduced and also evaluated the binding affinity of the hybrids to mycobacterial and antibacterial targets. These studies provide insights into the potential modes of action underlying the observed antimicrobial activity. This research holds significant promise, offering valuable insights into the development of novel antimicrobial agents.

## EXPERIMENTAL

All chemicals used in this study were procured from Sigma-Aldrich Co. (St. Louis, USA), Merck (Whitehouse Station, USA), Qualigens Fine Chemicals (Mumbai, India), Loba Chemie Pvt. Ltd. (Mumbai, India) and Himedia Laboratories Pvt. Ltd (Mumbai, India). Melting points of the synthesized compounds were determined using a digital melting point apparatus equipped with open capillary tubes and are uncorrected. Compound purity was evaluated through thin-layer chromatography (TLC) using pre-coated silica gel strips. A solvent system comprising a 2:1 ratio of hexane to ethyl acetate was employed and chromatographic spots were visualized using an ultraviolet chamber. Infrared spectra were recorded using a Shimadzu FT-IR 4000 instrument equipped with KBr disks. The CHNO elemental analysis was conducted using the Perkin-Elmer Series II 2400 CHNS/O Elemental Analyzer. This mass spectra were obtained using a JEOL GC mate II GC-mass spectrometer operating at 70 eV. The  $^1\text{H}$  NMR spectra were collected using a Bruker AVIII-500 MHz FT-NMR spectrometer. Tetramethylsilane served as the internal standard and DMSO was the preferred solvent.

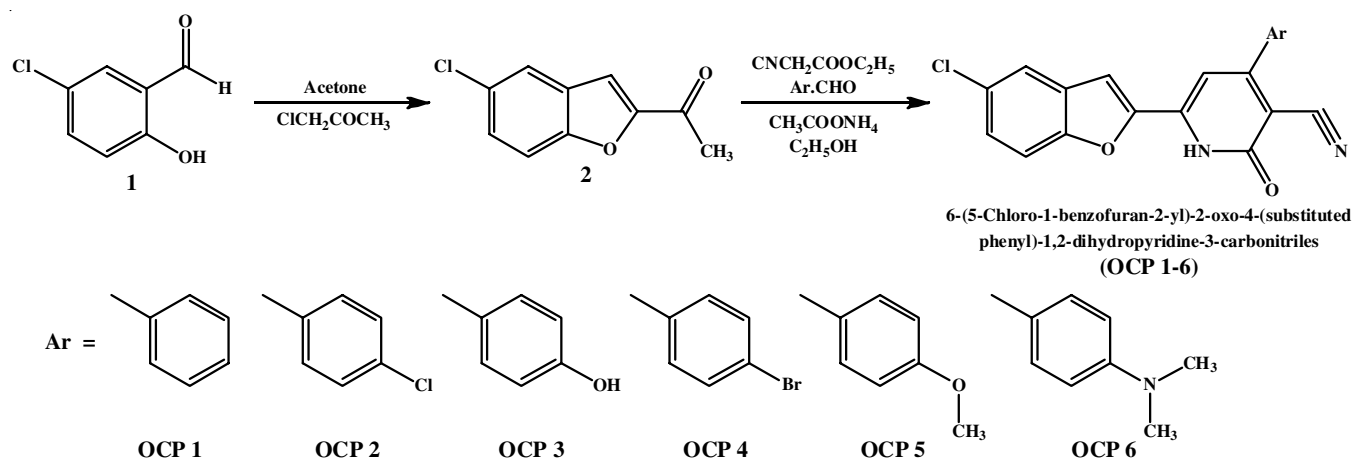
**Synthesis of 5-chloro-2-acetylbenzofuran (2):** A mixture containing 5-chlorosalicylaldehyde (**1**), chloroacetone (4.63 g,

0.05 mol) and anhydrous  $\text{K}_2\text{CO}_3$  (15 g) was gently refluxed in dry acetone (50 mL) for 12 h. After the completion of reaction, the reaction product was filtered and the filtrate was subjected to solvent removal under reduced pressure. This process yielded 5-chloro-2-acetylbenzofuran (**2**) as a light brownish solid. The obtained product was further purified by recrystallization from ethanol. Yield: 75%, m.p.: 83-85 °C. IR (KBr,  $\nu_{\text{max}}$ ,  $\text{cm}^{-1}$ ): 1666 (C=O), 1461 (C=C) and 790 (C-Cl), MS ( $m/z$ , %): 194 ( $\text{M}^+$ ) and 196 ( $\text{M}+2^+$ ),  $^1\text{H}$  NMR ( $\delta$  ppm): 7.2-7.8 (4Ar-H), 2.6 (3H, s,  $\text{CH}_3$ ).

**Synthesis of 6-(5-chloro-1-benzofuran-2-yl)-2-oxo-4-(substituted phenyl)-1,2-dihydropyridine-3-carbonitriles (OCP 1-6):** Condensation of various aromatic aldehydes (0.01 mol), 5-chloro-2-acetyl benzofuran (**2**) (1.94 g, 0.01 mol) and ethylcyanoacetate (1.13 g, 0.01 mol) in boiling ethanol (5 mL) with ammonium acetate (1.15 g, 0.01 mol) through refluxing for 4 h and then yielded 6-(5-chloro-1-benzofuran-2-yl)-2-oxo-4-(substituted phenyl)-1,2-dihydropyridine-3-carbonitriles (OCP 1-6). Following refluxing, the reaction mixture was cooled and the isolated solid product was collected *via* filtration (Scheme-I). Subsequent crystallization from ethanol ensured compound purity, confirmed by TLC using a hexane and ethyl acetate mixture as mobile phase.

**6-(5-Chloro-1-benzofuran-2-yl)-2-oxo-4-phenyl-1,2-dihydropyridine-3-carbonitrile (OCP1):** Yield: 75%; m.p.: 250-252 °C; FT-IR (KBr,  $\nu_{\text{max}}$ ,  $\text{cm}^{-1}$ ): 3342 (NH), 2245 (C $\equiv$ N), 1660 (C=O), 1458 (C=C), 800 (C-Cl);  $^1\text{H}$  NMR (DMSO- $d_6$ ,  $\delta$  ppm): 4.68 (1H, s, NH), 7.09 (1H, s), 7.41-7.88 (8H, 7.48 (d), 7.53 (d), 7.53 (d), 7.59 (d), 7.71 (t), 7.82 (d)), 8.33 (1H, d); MS ( $m/z$ , %): 346.05 ( $\text{M}^+$ ). Anal. calcd. (found) % for  $\text{C}_{20}\text{H}_{11}\text{N}_2\text{O}_2\text{Cl}$ : C, 69.27 (69.31); H, 3.20 (3.19); Cl, 10.22 (10.26); N, 8.08 (8.10); O, 9.23 (9.25).

**6-(5-Chloro-1-benzofuran-2-yl)-4-(4-chlorophenyl)-2-oxo-1,2-dihydropyridine-3-carbonitrile (OCP2):** Yield: 62%; m.p.: 244-246 °C; FT-IR (KBr,  $\nu_{\text{max}}$ ,  $\text{cm}^{-1}$ ): 3362 (NH), 2242 (C $\equiv$ N), 1663 (C=O), 1448 (C=C), 788 (C-Cl);  $^1\text{H}$  NMR (DMSO- $d_6$ ,  $\delta$  ppm): 4.42 (1H, s, NH), 7.07 (1H, s), 7.45 (1H, d), 7.52-7.72 (5H, 7.58 (d), 7.58 (d), 7.66 (d)), 7.82 (1H, d), 8.31 (1H, d); MS ( $m/z$ , %): 380.01 ( $\text{M}^+$ ). Anal. calcd. (found) % for  $\text{C}_{20}\text{H}_{10}\text{N}_2\text{O}_2\text{Cl}_2$ : C, 63.01 (63.05); H, 2.64 (2.68); Cl, 18.60 (18.62); N, 7.35 (7.38); O, 8.39 (8.45).



**6-(5-Chloro-1-benzofuran-2-yl)-4-(4-hydroxyphenyl)-2-oxo-1,2-dihydropyridine-3-carbonitrile (OCP3):** Yield: 65%; m.p.: 265-267 °C; FT-IR (KBr,  $\nu_{\max}$ ,  $\text{cm}^{-1}$ ): 3762 (OH), 3325 (NH), 2223 ( $\text{C}\equiv\text{N}$ ), 1665 ( $\text{C}=\text{O}$ ), 1452 ( $\text{C}=\text{C}$ ), 804 (C-Cl);  $^1\text{H}$  NMR (DMSO- $d_6$ ,  $\delta$  ppm): 4.65 (1H, s, NH), 6.89-7.10 (3H, 6.95 (d), 7.05 (s)), 7.38-7.62 (4H, 7.45 (d), 7.55 (d), 7.57 (d)), 7.81 (1H, d), 8.31 (1H, d), 9.6 (1H, s, OH); MS ( $m/z$ , %): 362.04 (M+). Anal. calcd. (found) % for  $\text{C}_{20}\text{H}_{11}\text{N}_2\text{O}_3\text{Cl}$ : C, 66.22 (66.20); H, 3.06 (3.09); Cl, 9.77 (9.74); N, 7.72 (7.75); O, 13.23 (13.26).

**6-(5-Chloro-1-benzofuran-2-yl)-4-(4-bromophenyl)-2-oxo-1,2-dihydropyridine-3-carbonitrile (OCP4):** Yield: 72%; m.p.: 300-302 °C; FT-IR (KBr,  $\nu_{\max}$ ,  $\text{cm}^{-1}$ ): 3328 (NH), 2252 ( $\text{C}\equiv\text{N}$ ), 1662 ( $\text{C}=\text{O}$ ), 1459 ( $\text{C}=\text{C}$ ), 547 (C-Br), 802 (C-Cl);  $^1\text{H}$  NMR (DMSO- $d_6$ ,  $\delta$  ppm): 4.68 (1H, s, NH), 7.06 (1H, s), 7.39-7.70 (6H, 7.45 (d), 7.47 (d), 7.58 (d), 7.63 (d)), 7.82 (1H, d), 8.31 (1H, d); MS ( $m/z$ , %): 423.96 (M+). Anal. calcd. (found) % for  $\text{C}_{20}\text{H}_{10}\text{N}_2\text{O}_2\text{BrCl}$ : C, 56.43 (56.45); H, 2.37 (2.39); Br, 18.77 (18.82); Cl, 8.33 (8.36); N, 6.58 (6.61); O, 7.52 (7.55).

**6-(5-Chloro-1-benzofuran-2-yl)-4-(4-methoxyphenyl)-2-oxo-1,2-dihydropyridine-3-carbonitrile (OCP5):** Yield: 58%; m.p.: 275-277 °C; FT-IR (KBr,  $\nu_{\max}$ ,  $\text{cm}^{-1}$ ): 3350 (NH), 2206 ( $\text{C}\equiv\text{N}$ ), 1668 ( $\text{C}=\text{O}$ ), 1450 ( $\text{C}=\text{C}$ ), 811 (C-Cl);  $^1\text{H}$  NMR (DMSO- $d_6$ ,  $\delta$  ppm): 3.88 (3H, s,  $\text{OCH}_3$ ), 4.9 (1H, s, NH), 7.05 (1H, s), 7.21 (2H, d), 7.45 (1H, d), 7.52-7.72 (3H, 7.57 (d), 7.66 (d), 7.81 (1H, d), 8.31 (1H, d); MS ( $m/z$ , %): 376.06 (M+). Anal. calcd. (found) % for  $\text{C}_{21}\text{H}_{13}\text{ClN}_2\text{O}_3$ : C, 66.94 (66.97); H, 3.48 (3.50); Cl, 9.41 (9.44); N, 7.43 (7.47); O, 12.74 (12.78).

**6-(5-Chloro-1-benzofuran-2-yl)-4-[4-(dimethylamino)phenyl]-2-oxo-1,2-dihydropyridine-3-carbonitrile (OCP6):** Yield: 60%; m.p.: 251-253 °C; FT-IR (KBr,  $\nu_{\max}$ ,  $\text{cm}^{-1}$ ): 3354 (NH), 2253 ( $\text{C}\equiv\text{N}$ ), 1681 ( $\text{C}=\text{O}$ ), 1455 ( $\text{C}=\text{C}$ ), 780 (C-Cl);  $^1\text{H}$  NMR (DMSO- $d_6$ ,  $\delta$  ppm): 2.91 (6H, s), 6.62 (2H, d), 7.00 (1H, s), 7.38-7.60 (2H, 7.44 (d), 7.55 (d)), 7.63-7.87 (3H, 7.69 (d), 7.81 (d)), 8.29 (1H, d); MS ( $m/z$ , %): 389.09 (M+). Anal. calcd. (found) % for  $\text{C}_{22}\text{H}_{16}\text{N}_3\text{O}_2\text{Cl}$ : C, 67.78 (67.81); H, 4.14 (4.17); Cl, 9.09 (9.14); N, 10.78 (10.82); O, 8.21 (8.24).

**Biological activity:** The title compounds underwent pharmacological activity prediction using the online tool PASS. This advanced system compares their structures with well-established biologically active substances, predicting potential pharmacological properties that can later be confirmed through experiments. PASS boasts a vast database, incorporating thousands of substances from the training set, facilitating an objective estimation of potential biological activities. Notably, it requires only the structural formula or SMILES of the chemical compound, making it applicable at an early stage of investigation [27]. Upon submitting the structures of the title compounds to the PASS online program, diverse potential mechanisms of action and biological activities were predicted.

**Syntelly:** Syntelly, an artificial intelligence platform for organic and medicinal chemistry, offers rapid access to experimental data and predicts properties of over 150 million organic compounds. It includes a visual module for exploring chemical space and generating structures with predefined properties. The primary database serves as a hub for searching molecules by inputting names in various formats. A traffic light system on the molecule card compares safety parameters, covering toxicity,

physico-chemical attributes, biological characteristics and environmental properties [28].

**PLATO:** Polypharmacology pLATform predictiOn (PLATO) is a user-friendly web platform for drug discovery, serving the dual purpose of identifying potential protein drug targets and calculating bioactivity values for small molecules. Predictions are based on the similarity principle, employing reverse ligand-based screening with a dataset of 632,119 compounds known to be experimentally active on 6004 protein targets. The efficient backend implementation ensures speedy results, typically returned in less than 20 seconds. The intuitive graphical user interface allows for easy input and the transparent output is presented in a standard portable document format report [29].

### Dual target docking studies

**Preparation of target molecules:** To prepare the target molecules, a dual-target docking study was conducted using the GLIDE docking program (Schrödinger 2020-1) [30]. The synthesized compounds (OCP 1-6) underwent docking within the active sites of two crystal structures *viz.* *Mycobacterium tuberculosis* enoyl-ACP reductase (PDB code: 2PR2) and *Escherichia coli* Topoisomerase IV ParE 24kDa subunit (PDB code: 1S14). The quality of the target protein structures was rigorously assessed using tools such as ERRAT, Verify 3D and the Structural Analysis and Verification Server [31-33]. These analyses confirmed the acceptability and high quality of all protein models. Furthermore, a detailed analysis of the Ramachandran plot was conducted using RAMPAGE to evaluate dihedral angles and permissible conformations [34].

**Preparation of ligand molecules:** In the process of preparing ligand molecules, the 2D chemical structures of compounds **OCP 1-6** were initially drawn using ChemDraw Ultra Version 8.0.3 [35] and saved in binary format. Subsequently, these structures were converted into the SDF format using the Open Babel GUI version 2.4.1, a versatile virtual screening tool designed for Windows [36,37]. Following that, a thorough energy minimization was performed using the OPLS3e force field with Ligprep. This process included ionization at a target pH of 7.0  $\pm$  2.0, desalting and the preservation of specified chiralities [38]. To facilitate a comparative assessment of binding affinities, ATP was employed as reference ligand in the docking experiments. The results were comprehensively evaluated by examining binding interactions and docking scores obtained from GLIDE\_SP ligand docking.

**Antitubercular activity:** The synthesized 6-(5-chloro-1-benzofuran-2-yl)-2-oxo-4-(substitutedphenyl)-1,2-dihydropyridine-3-carbonitriles (**OCP 1-6**) underwent screening for antitubercular activity using the microplate Alamar blue assay method (MABA). Each compound was tested against the *M. tuberculosis* H37 RV strain, with isonicotinic acid hydrazide (INH) as the standard drug for comparison. For the assay setup, 200  $\mu\text{L}$  of sterile deionized water was added to the outermost wells of a sterile 96-well plate to prevent medium evaporation during incubation. Subsequently, 100  $\mu\text{L}$  of Middlebrook 7H9 (MB 7H9) broth was dispensed into the wells and the synthesized compounds were serially diluted directly on the plate.

The antitubercular activity was assessed at final drug concentrations of 0.2, 0.4, 0.8, 1.6, 3.125, 6.25, 12.5, 25, 50 and 100  $\mu\text{g/mL}$ .

The plates were covered, sealed with parafilm and incubated at 37 °C for 5 days. After the incubation period, 25  $\mu\text{L}$  of freshly prepared 1:1 mixture of Alamar blue reagent and 10% Tween 80 was added to each well. The plates underwent an additional 24 h incubation. Interpretation of the results was based on the observed color change in the wells: a blue colour indicated no mycobacterial growth, while a pink colour signified mycobacterial growth [39].

**Antibacterial activity:** The antibacterial activity of the synthesized compounds (**OCP 1-6**) was assessed using the agar cup plate method against a spectrum of bacteria, including Gram-negative organisms like *Escherichia coli* and *Pseudomonas aeruginosa*, as well as Gram-positive organisms, such as *Bacillus subtilis* and *Staphylococcus epidermatitis*. Evaluation was conducted *via* the minimum inhibitory concentration (MIC) method, with ciprofloxacin as reference standard.

In the procedure, brain heart infusion agar was brought to room temperature and colonies were transferred to the plates. Their turbidity was visually adjusted to match a 0.5 McFarland turbidity standard. Swabbing the entire agar plate surface three times, with a 60° rotation between each streaking, ensured the uniform distribution. After allowing the inoculated plate to stand for at least 5 min, a 5 mm hollow tube was pressed onto the agar, creating five wells. Then, 75, 50, 25, 10 and 5  $\mu\text{L}$  of the synthesized compounds were added to the respective wells. After 24 h of incubation at 37 °C, the inhibition zone diameter was measured in mm. The MIC procedure involved repeating serial dilution up to a  $10^{-9}$  dilution for each synthesized compound [40,41].

## RESULTS AND DISCUSSION

Among the various reported methods for synthesizing 3-cyano-2-oxa-pyridines [42], the present research makes a notable contribution through an efficient one-pot multi-component reaction method. The literature recommends condensation of chalcone with ethyl cyanoacetate and ammonium acetate to synthesize these chemicals, although this approach is time-consuming [43]. In present work, we employed a solvent-based one-pot multi-component reaction, offering a quicker and more practical alternative.

The purity of the synthesized compounds, including **2** and **OCP 1-6**, was verified through TLC using a mobile phase composed of hexane and ethyl acetate mixture. Confirmation of their identity was established by the presence of a single spot on TLC, well-defined melting points and distinctive spectral features. The infrared spectra of the synthesized compounds (**OCP 1-6**), distinctive bands were observed around 3350, 2240 and 1660  $\text{cm}^{-1}$ , confirming the presence of N-H, CN and C=O bonds within the oxacyanopyridine ring. These observations signify the successful formation of the target compounds. The  $^1\text{H}$  NMR spectra of these synthesized compounds revealed signals for aromatic protons resonating within the range of  $\delta$  7.1 to 8.0 ppm. Additionally, the signals for the characteristic dihydropyridine -NH group were observed around  $\delta$  4.0 ppm.

Notably, compound **OCP 3** exhibited a proton singlet at  $\delta$  9.6 ppm, corresponding to the proton of the hydroxy group located at the *para* position of phenyl ring attached to the 4<sup>th</sup> position of the dihydropyridine ring system. Mass spectrometry analysis further validated the presence of the expected molecular ion peak ( $\text{M}^+$ ) fragments for the synthesized compounds.

**Prediction of biological activity:** Table-1 presents PASS-predicted biological activity profiles based on an extensive training dataset of 60,000 biologically active compounds across 4,500 distinct activities. Calculated probabilities ( $\text{P}_a$  and  $\text{P}_i$ ) indicate specific activity likelihood. Initially, all the synthesized compounds were projected to exhibit antitubercular and antibacterial activities with  $\text{P}_a$  values below 0.5. However, the experimental assessments contradicted these predictions, revealing significant antitubercular and antibacterial activities, challenging PASS's forecasts. In summary, PASS predicts promising the pharmacological potential for these compounds, especially in antitubercular and antibacterial contexts. The subsequent experiments can validate these predictions, exploring their potential as novel pharmacologically active substances.

**Toxicity properties predicted by syntelly:** The utilization of computational models, as proposed by various researchers, emerges as an effective strategy to reduce drug attrition due to toxicity, providing a valuable tool for decision-making across diverse industries. As reported by Sharma *et al.* [44] toxicity prediction plays a crucial role in supporting the development of safer drugs, minimizing environmental impact and contributing to public health. Table-2 provides an overview of the predicted toxicity properties of the synthesized compounds using Syntelly software. Specifically, the blood-brain barrier permeability of the synthesized compounds **OCP 1-6** was assessed, with compound **OCP-3** being predicted to be impermeable. Importantly, all compounds exhibited safety in terms of cardiotoxicity, mutagenicity and carcinogenicity. However, the predictions highlighted potential hepatotoxic and reproductive toxic characteristics for these synthesized compounds.

**Quantitative bioactivity profiling by PLATO:** The quantitative bioactivity profiling by PLATO (Polypharmacology pLATform predictiOn) holds significant value in drug discovery and development. This approach allows researchers to comprehensively assess the interactions of potential drug candidates with a wide range of biological targets [45].

The polypharmacological effects of the synthesized compounds (**OCP 1-6**) are summarized in Table-3. Notably, all compounds, with the exception of **OCP-2**, were predicted to interact with *M. tuberculosis* targets. Additionally, they exhibited some potential interactions with bacteria, viruses and other pathogenic microbial targets. This observation underscores their potential as antimicrobial agents, particularly against *M. tuberculosis* targets. However, it is essential to acknowledge that these compounds also demonstrated off-target interactions with human targets, signaling a need for caution due to potential adverse effects or the possibility of engaging in other significant biological activities. A comprehensive understanding of these polypharmacological effects is crucial for informed decision making in the development of these compounds as potential therapeutics.

TABLE-1  
PREDICTED BIOLOGICAL ACTIVITY SPECTRUM OF SYNTHESIZED COMPOUNDS (OCP 1-6)

Compound	Pa	Pi	Activity
OCP 1	0.627	0.018	Kinase inhibitor
	0.194	0.181	Antimycobacterial
	0.050	0.020	Enoyl-[acyl-carrier-protein] reductase (NADH) inhibitor
	0.119	0.108	Bacterial efflux pump inhibitor
OCP 2	0.623	0.018	Kinase inhibitor
	0.196	0.178	Antimycobacterial
	0.051	0.020	Enoyl-[acyl-carrier-protein] reductase (NADH) inhibitor
	0.120	0.104	Bacterial efflux pump inhibitor
OCP 3	0.634	0.017	Kinase inhibitor
	0.612	0.011	CYP1A1 substrate
	0.208	0.163	Antimycobacterial
	0.059	0.011	Enoyl-[acyl-carrier-protein] reductase (NADH) inhibitor
OCP 4	0.503	0.034	Kinase inhibitor
	0.206	0.162	Antituberculosic
	0.263	0.107	Antimycobacterial
	0.041	0.041	Enoyl-[acyl-carrier-protein] reductase (NADH) inhibitor
OCP 5	0.584	0.022	Kinase inhibitor
	0.197	0.177	Antimycobacterial
	0.133	0.050	Bacterial efflux pump inhibitor
	0.045	0.030	Enoyl-[acyl-carrier-protein] reductase (NADH) inhibitor
OCP 6	0.539	0.022	CYP1A substrate
	0.489	0.037	Kinase inhibitor
	0.336	0.010	Cell wall biosynthesis inhibitor
	0.044	0.031	Enoyl-[acyl-carrier-protein] reductase (NADH) inhibitor
Isoniazid	0.810	0.003	Antituberculosic
	0.798	0.004	Antimycobacterial
	0.371	0.038	Antibacterial
	0.226	0.042	Trans-2-enoyl-CoA reductase (NAD <sup>+</sup> ) inhibitor
Ciprofloxacin	0.639	0.008	Antimycobacterial
	0.588	0.009	Antibacterial
	0.452	0.019	Antituberculosic
	0.304	0.086	Antiviral (Adenovirus)

TABLE-2  
PREDICTIVE TOXICITY PROPERTIES USING SYNTTELLY

Compound	Blood brain barrier permeability	Cardiotoxicity	Mutagenicity	Carcinogenicity	Hepatotoxicity	Reproductive toxicity
OCP 1	YES	No	No	No	YES	YES
OCP 2	YES	No	No	No	YES	YES
OCP 3	No	No	No	No	YES	YES
OCP 4	YES	No	No	No	YES	YES
OCP 5	YES	No	No	No	YES	YES
OCP 6	YES	No	No	No	YES	YES
Isoniazid	No	No	YES	No	YES	YES
Ciprofloxacin	No	No	YES	No	YES	YES

**Dual target docking studies:** The effectiveness of molecular docking in drug discovery is evident in its ability to provide valuable insights into ligand-receptor interactions, facilitating the rational design of therapeutic agents [46,47]. Before embarking on docking studies, the assurance of target protein quality is paramount. The assessment of 3D models using RAMPAGE, a tool employing Ramachandran plot calculations, confirmed the reliability and accuracy of the predicted protein structures (Fig. 1). High percentages in the favoured and allowed regions for both 2PR2 and 1S14 suggested excellent model quality [48,49]. Further validation using ERRAT and verify 3D [50] reinforced the quality of the target protein models, with ERRAT

analysis yielding quality factors exceeding the 95% rejection limit. Verify 3D analysis provided additional insights into the structurally acceptable environment of the models, with non-negative scores for all amino acids in 2PR2 and a majority in 1S14 (Fig. 2).

Glide, a reputable Schrödinger docking software, was employed to predict docking scores for each ligand against both target proteins [51]. Visual representations in Figs. 3 and 4 displayed the docking of compounds OCP 1-6, with OCP-4 achieving the highest docking score. Importantly, all compounds exhibited promising docking scores comparable to their respective standards.

TABLE-3  
QUANTITATIVE BIOACTIVITY PROFILING USING PLATO

Compound	Target	Source	IC <sub>50</sub> <sup>a</sup>	EC <sub>50</sub> <sup>b</sup>
<b>OCP 1</b>	Serine/threonine-protein kinase PIM1	Homo sapiens	24.6 nM	264nM
	Monoamine oxidase B	Homo sapiens	868 nM	6.29 μM
	Thymidine phosphorylase	<i>Escherichia coli</i> K-12	14.2 μM	–
	Thymidylate kinase	<i>Mycobacterium tuberculosis</i>	302 nM	–
<b>OCP 2</b>	Human immunodeficiency virus type 1 reverse transcriptase	Human immunodeficiency virus 1	614 nM	298 nM
	Cannabinoid CB1 receptor	Homo sapiens	60.8 nM	177 nM
	Streptokinase A	<i>Streptococcus pyogenes</i>	–	3.82 μM
	Thymidine phosphorylase	<i>Escherichia coli</i> K-12	14.1 μM	–
<b>OCP 3</b>	Matrix metalloproteinase 13	Homo sapiens	29.3 nM	–
	Enoyl-acyl-carrier protein reductase	<i>Plasmodium falciparum</i>	2.54 μM	–
	Phosphotyrosine protein phosphatase	<i>Mycobacterium tuberculosis</i>	4.83 μM	–
	Thymidylate kinase	<i>Mycobacterium tuberculosis</i>	210 nM	–
<b>OCP 4</b>	Induced myeloid leukemia cell differentiation protein Mcl-1	Homo sapiens	3.55 μM	2.85 μM
	Hepatitis C virus NS5B RNA-dependent RNA polymerase	Hepatitis C virus	916 nM	142 nM
	Thymidine phosphorylase	<i>Escherichia coli</i> K-12	13.7 μM	–
	Thymidylate kinase	<i>Mycobacterium tuberculosis</i>	258 nM	–
<b>OCP 5</b>	Cannabinoid CB1 receptor	Homo sapiens	67.3 nM	177 nM
	Hepatitis C virus NS5B RNA-dependent RNA polymerase	Hepatitis C virus	906 nM	142 nM
	Enoyl-acyl-carrier protein reductase	<i>Plasmodium falciparum</i>	2.60 μM	–
	Thymidylate kinase	<i>Mycobacterium tuberculosis</i>	259 nM	–
<b>OCP 6</b>	Induced myeloid leukemia cell differentiation protein Mcl-1	Homo sapiens	3.46 μM	2.86 μM
	Hepatitis C virus NS5B RNA-dependent RNA polymerase	Hepatitis C virus	855 nM	130 nM
	Streptokinase A	<i>Streptococcus pyogenes</i>	3.83 μM	–
	Thymidylate kinase	<i>Mycobacterium tuberculosis</i>	256 nM	–

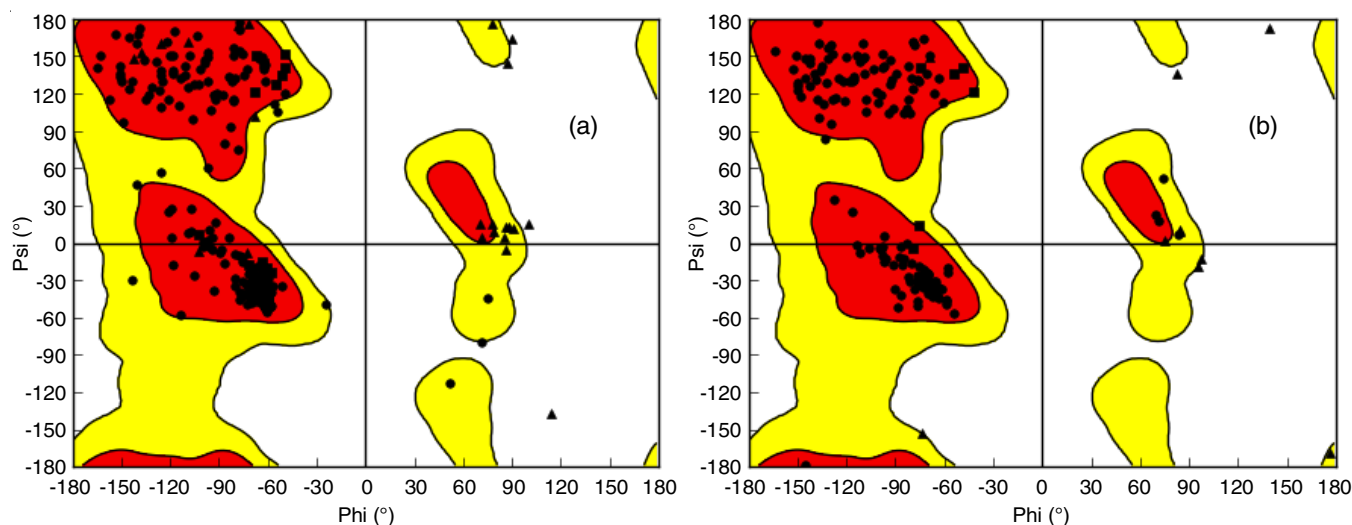


Fig. 1. Ramachandran plots generated *via* RAMPAGE for (a) 2PR2 and (b) 1S14; Residues in favoured (red), allowed (yellow) and outlier regions (white)

The interactions between the synthesized compounds (**OCP 1-6**) and the amino acid residues of target proteins 2PR2 and 1S14 were elucidated. All the synthesized compounds, except for **OCP-2** and **6**, demonstrated both hydrogen bond and hydrophobic interactions with 2PR2 (Table-4). Moreover, compounds **OCP-1, 3, 4** and **5** exhibited the hydrophobic interactions similar to the standard drug isoniazid (INH), albeit at different interaction sites. Additionally, compound **OCP-3** shares the same hydrogen bond interaction site (GLY 96) with the standard drug. With nearly equivalent binding affinities, as indicated by docking scores close to the standard score and insights from dual-target docking studies, these findings underscore the potential therapeutic relevance of the synthesized compounds.

The absence of hydrophobic interactions with the 1S14 target protein observed in the synthesized compounds highlights the need for a meticulous examination of their molecular design, structural features and potential optimization strategies. Employing both experimental and computational approaches will be essential to address these challenges and guide the refinement of the synthesized compounds, aiming for enhanced interactions with the target protein.

**Antimicrobial activity:** The antitubercular and antibacterial activities of all synthesized compounds (**OCP 1-6**) were systematically evaluated. In particular, the antitubercular activity of the synthesized oxacyanopyridines (**OCP 1-6**) was assessed against *M. tuberculosis* H37Rv in Middlebrook 7H9



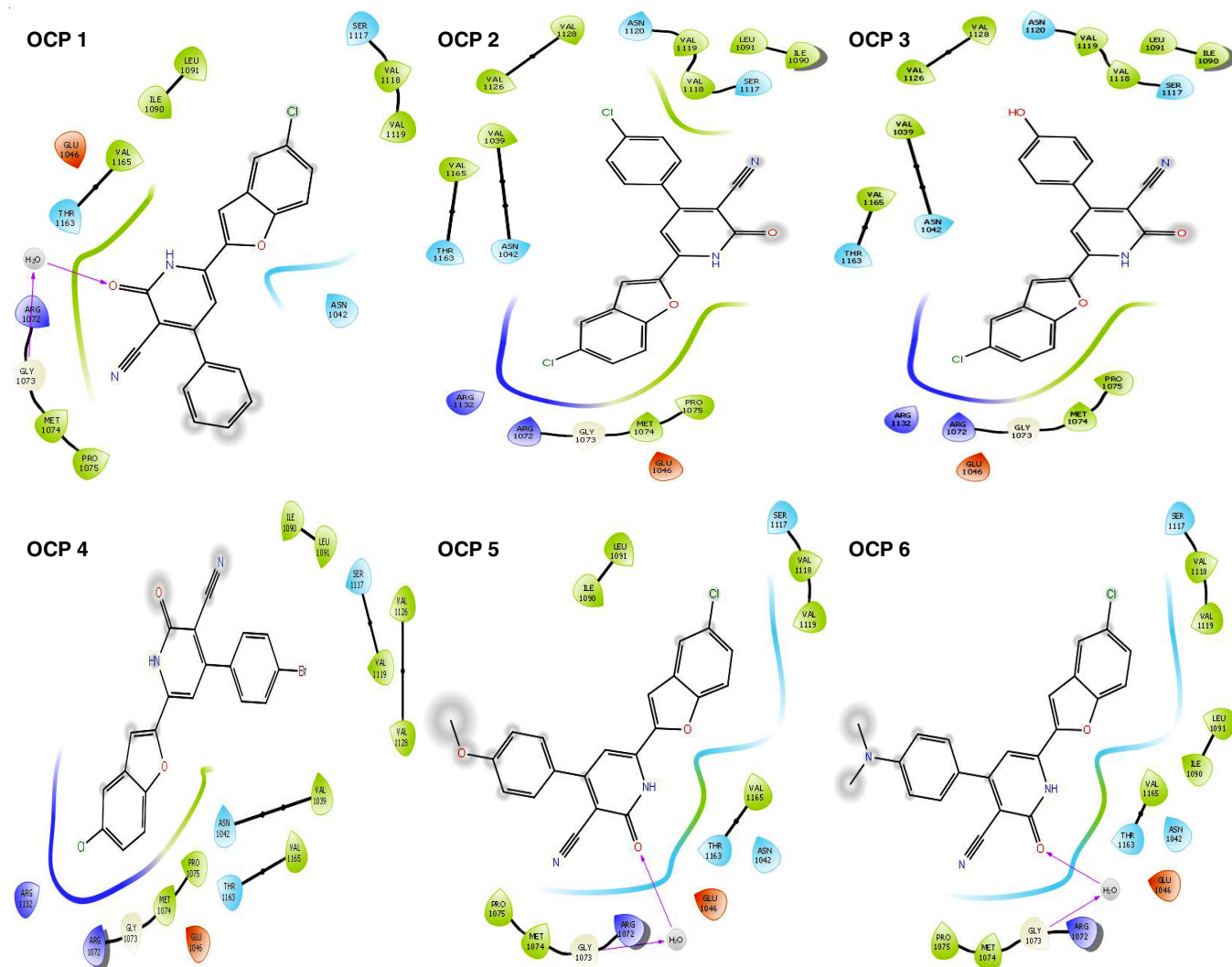
Fig. 4. Docking of oxacyanopyridine-benzofuran hybrids (**OCP 1-6**) with 1S14 protein

TABLE-4  
DOCKING SCORE AND MOLECULAR INTERACTION OF OXACYANOPYRIDINE-BENZOFURAN HYBRIDS (**OCP 1-6**) WITH 2PR2 AND 1S14 PROTEINS

Compound	2PR2 protein			1S14 protein		
	Docking score	H-Bond interactions	Hydrophobic interactions	Docking score	H-Bond interactions	Hydrophobic interactions
<b>OCP 1</b>	-8.428	THR 196	PHE 149	-5.657	GLY 1073	—
<b>OCP 2</b>	-7.147	LYS 165	—	-6.611	—	—
<b>OCP 3</b>	-8.706	GLY 96, MET 98	PHE 149	-6.406	—	—
<b>OCP 4</b>	-6.797	LYS 165	PHE 149	-5.408	—	—
<b>OCP 5</b>	-8.245	MET 98, THR 196	PHE 149	-5.631	GLY 1073	—
<b>OCP 6</b>	-8.208	—	—	-5.622	GLY 1073	—
Isoniazid	-7.244	VAL 95, GLY 96	PHE 41	—	—	—
Ciprofloxacin	—	—	—	-7.066	ASP 1069, GLY 1073	VAL 1118

broth media (MB 7H9 broth), with isoniazid (INH) serving as standard drug (Table-5).

Results from the antitubercular activity screening revealed distinct behaviour among the synthesized compounds. Notably, compounds **OCP-2, 4 and 5**, featuring *p*-chloro, *p*-bromo and *p*-methoxy groups on the aromatic moiety at the 4<sup>th</sup> position of dihydropyridine ring, respectively, exhibited activity at

concentrations of 25, 50 and 100 µg/mL. In contrast, the remaining compounds (**OCP 1 and 6**) exhibited no activity at any concentration, with the exception of compound **OCP-3**, which showed activity at concentrations of 50 and 100 µg/mL.

In interpreting these results, a thorough exploration of the structure-activity relationship (SAR) within the synthesized compounds is essential. The observed variations in the activity

TABLE-5  
ANTI-TUBERCULAR ACTIVITY OF  
OXACYANOPYRIDINE-BENZOFURAN HYBRIDS (OCP 1-6)

Compound	Minimum inhibitory concentration		
	25 µg/mL	50 µg/mL	100 µg/mL
OCP 1	R	R	R
OCP 2	S	S	S
OCP 3	R	S	S
OCP 4	S	S	S
OCP 5	S	S	S
OCP 6	R	R	R
Isoniazid	S	S	S

levels can be ascribed to specific structural features or substituent effects. In particular, halogens at the *para*-position of the phenyl ring at the 4<sup>th</sup> position of dihydropyridine stand out as electron-modulating groups that are good for antitubercular activity. The presence of halogens at the *para* position seems to exert a modulatory effect on the antitubercular properties of the synthesized compounds. This electron modulation may contribute to enhanced interactions with the target, potentially influencing the biological activity. Furthermore, a comparative analysis with the standard drug, isoniazid, provides valuable insights into the relative efficacy of the synthesized compounds in the context of antitubercular activity. The favourable effects observed with specific structural modifications, particularly the introduction of electron modulating groups, suggest a promising avenue for further optimization.

In the assessment of antibacterial activity using the agar cup-plate method, all the synthesized compounds (OCP 1-6) were tested, with ciprofloxacin as reference standard. The antibacterial activity demonstrated at 100 µg was remarkable, exhibiting the effectiveness similar to the reference standard, ciprofloxacin (Fig. 5). Specifically, compounds OCP-2, 3, 4 and 5, featuring *p*-chlorophenyl, *p*-hydroxyphenyl, *p*-bromophenyl and *p*-methoxyphenyl group at the 4<sup>th</sup> position of the dihydropyridine ring, respectively, displayed a significant activity. In contrast, the remaining compounds (OCP-1 and 6) exhibited relatively less activity.

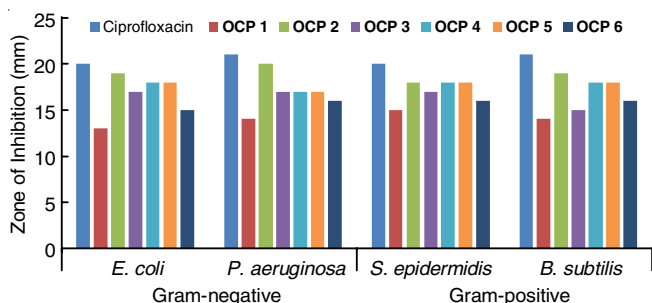


Fig. 5. Antibacterial activity of oxacyanopyridine-benzofuran hybrids (OCP 1-6)

The observed variations in activity levels can be attributed to specific structural features or substituent effects within the compounds. The electron-modulating groups, such as halogens at the *para* position of the phenyl ring located at the 4<sup>th</sup> position of dihydropyridine, were found to be favourable for both antibacterial and antitubercular activities. This consistent trend

across different biological activities suggests that these synthesized compounds possess substantial potential as broad spectrum antimicrobial agents. These findings emphasize the promising avenue for the development of novel antibacterial agents, further accentuating the versatility and potential clinical significance of the synthesized compounds.

## Conclusion

This work introduces an innovative approach for the synthesis of 3-cyano-2-oxa-pyridines, a class of compounds with diverse applications. This study successfully achieved the synthesis and characterization of a novel series of oxacyano pyridine hybrids (OCP 1-6). Starting from 5-chlorosalicylaldehyde, a meticulous multistep synthetic strategy was employed, integrating pyridine and benzofuran motifs into the molecular structure. Utilizing computational tools, the research predicted diverse pharmacological properties of the synthesized hybrids, encompassing antitubercular and antibacterial activities, toxicity profiles and potential molecular targets. *In vitro* assessments, complemented by Schrödinger docking simulations, provided insights into the efficacy of the synthesized compounds against *Mycobacterium tuberculosis* enoyl-ACP reductase and *E. coli* Topoisomerase IV. The antitubercular and antibacterial evaluations highlighted the significant activity of compounds OCP-2, 3, 4 and 5 suggesting their potential as promising agents against these microbial strains. The structure-activity relationship (SAR) analysis emphasized the impact of specific structural features, particularly electron-modulating groups, on the observed biological activities.

## ACKNOWLEDGEMENTS

The authors are grateful for the research support from Sri Padmavathi School of Pharmacy, Andhra University and Mohan Babu University. Additionally, the authors also extended their appreciation to the authorities of PASS, Syntelly and PLATO for generously providing free softwares.

## CONFLICT OF INTEREST

The authors declare that there is no conflict of interests regarding the publication of this article.

## REFERENCES

- K.U. Sadek, R.A. Mekheimer, M. Abd-Elmonem, F.A. Abo-Elsoud, A.M. Hayallah, S.M. Mostafa, M.H. Abdellatif, M.A.S. Abourehab, T.A. Farghaly and A. Elkamhawy, *J. Mol. Struct.*, **1286**, 135616 (2023); <https://doi.org/10.1016/j.molstruc.2023.135616>
- M.I. Ali and M.M. Naseer, *RSC Adv.*, **13**, 30462 (2023); <https://doi.org/10.1039/D3RA05953G>
- K. Vaithegi, S. Yi, J.H. Lee, B.V. Varun and S.B. Park, *Commun. Chem.*, **6**, 112 (2023); <https://doi.org/10.1038/s42004-023-00914-5>
- M.B. Islam, M.I. Islam, N. Nath, T.B. Emran, M.R. Rahman, R. Sharma and M.M. Matin, *Biomed Res Int.*, **2023**, 9967591 (2023); <https://doi.org/10.1155/2023/9967591>
- A.F. Villamizar-Mogotocoro, L.Y. Vargas-Méndez and V.V. Kouznetsov, *Eur. J. Pharm. Sci.*, **151**, 105374 (2020); <https://doi.org/10.1016/j.ejps.2020.105374>
- W. Jiang, W. Cheng, T. Zhang, T. Lu, J. Wang, Y. Yan, X. Tang and X. Wang, *J. Mol. Struct.*, **1270**, 133901 (2022); <https://doi.org/10.1016/j.molstruc.2022.133901>

7. M. Alrooqi, S. Khan, F.A. Alhumaydhi, S.A. Asiri, M. Alshamrani, M.M. Mashraqi, A. Alzamami, A.M. Alshahrani and A.A. Aldahish, *Anticancer. Agents Med. Chem.*, **22**, 2775 (2022); <https://doi.org/10.2174/1871520622666220324102849>
8. V. Kamat, R. Santosh, B. Poojary, S.P. Nayak, M. Sankaranarayanan, B.K. Kumar, Faheem, S. Khanapure, D.A. Barretto and S.K. Vootla, *ACS Omega*, **5**, 25228 (2020); <https://doi.org/10.1021/acsomega.0c03386>
9. M. Marinescu and C.V. Popa, *Int. J. Mol. Sci.*, **23**, 5659 (2022); <https://doi.org/10.3390/ijms23105659>
10. F. Manna, F. Chimenti, A. Bolasco, A. Filippelli, A. Palla, W. Filippelli, E. Lampa and R. Mercantini, *Eur. J. Med. Chem.*, **27**, 627 (1992); [https://doi.org/10.1016/0223-5234\(92\)90141-M](https://doi.org/10.1016/0223-5234(92)90141-M)
11. Z. Xu, S. Zhao, Z. Lv, L. Feng, Y. Wang, F. Zhang, L. Bai and J. Deng, *Eur. J. Med. Chem.*, **162**, 266 (2019); <https://doi.org/10.1016/j.ejmech.2018.11.025>
12. Z. Xu, S. Zhao, Z. Lv, L. Feng, Y. Wang, F. Zhang, L. Bai and J. Deng, *Eur. J. Med. Chem.*, **162**, 266 (2019); <https://doi.org/10.1016/j.ejmech.2018.11.025>
13. B.V. Lichitsky, V.G. Melekina, A.N. Komogortsev, V.A. Migulin, Y.V. Nelyubina, A.N. Fakhrutdinov, E.D. Daeva and A.A. Dudinov, *Tetrahedron*, **83**, 131980 (2021); <https://doi.org/10.1016/j.tet.2021.131980>
14. B.V. Lichitsky, T.T. Karibov, A.N. Komogortsev and V.G. Melekina, *Tetrahedron*, **132**, 133244 (2023); <https://doi.org/10.1016/j.tet.2022.133244>
15. D. Dwarakanath and S.L. Gaonkar, *Asian J. Org. Chem.*, **11**, e202200282 (2022); <https://doi.org/10.1002/ajoc.202200282>
16. Z. Xu, D. Xu, W. Zhou and X. Zhang, *Curr. Top. Med. Chem.*, **22**, 64 (2022); <https://doi.org/10.2174/1568026621666211122162439>
17. A.M. Srour, S.S. Abd El-Karim, D.O. Saleh, W.I. El-Eraky and Z.M. Nofal, *Bioorg. Med. Chem. Lett.*, **26**, 2557 (2016); <https://doi.org/10.1016/j.bmcl.2016.03.054>
18. E.M. Keshk, *Heteroatom Chem.*, **15**, 85 (2004); <https://doi.org/10.1002/hc.10219>
19. T. Zawadowski and C. Wiercińska-Radzio, *Acta Pol. Pharm.*, **43**, 207 (1986).
20. P. Martins, J. Jesus, S. Santos, L.R. Raposo, C. Roma-Rodrigues, P.V. Baptista and A.R. Fernandes, *Molecules*, **20**, 16852 (2015); <https://doi.org/10.3390/molecules200916852>
21. S.S.A. El-Karim, A.H. Mahmoud, A.K. Al-Mokaddem, N.E. Ibrahim, H.M. Alkahtani, A.A. Zen and M.M. Anwar, *Molecules*, **28**, 6814 (2023); <https://doi.org/10.3390/molecules28196814>
22. K. Vaithegi, S. Yi, J.H. Lee, B.V. Varun and S.B. Park, *Commun. Chem.*, **6**, 112 (2023); <https://doi.org/10.1038/s42004-023-00914-5>
23. TB/COVID-19 Global Study Group, *Eur. Respir. J.*, **59**, 2102538 (2022); <https://doi.org/10.1183/13993003.02538-2021>
24. T. Shah, Z. Shah, N. Yasmeen, Z. Baloch and X. Xia, *Front. Immunol.*, **13**, 909011 (2022); <https://doi.org/10.3389/fimmu.2022.909011>
25. P. Daneshvar, B. Hajikhani, F. Sameni, N. Noorisephr, N. Bostanshirin, F. Zare, S. Yazdani, M. Goudarzi, S. Sayyari and M. Dadashi, *Heliyon*, **9**, e13637 (2023); <https://doi.org/10.1016/j.heliyon.2023.e13637>
26. A.V. Sadybekov and V. Katritch, *Nature*, **616**, 673 (2023); <https://doi.org/10.1038/s41586-023-05905-z>
27. D.A. Filimonov, A.A. Lagunin, T.A. Glorizova, D.S. Druzhilovskii, A.V. Rudik, P.V. Pogodin and V.V. Poroikov, *Chem. Heterocycl. Compd.*, **50**, 444 (2014); <https://doi.org/10.1007/s10593-014-1496-1>
28. L. Krasnov, I. Khokhlov, M.V. Fedorov and S. Sosnin, *Sci. Rep.*, **11**, 14798 (2021); <https://doi.org/10.1038/s41598-021-94082-y>
29. F. Ciriaco, N. Gambacorta, D. Trisciuzzi and O. Nicolotti, *Int. J. Mol. Sci.*, **23**, 5245 (2022); <https://doi.org/10.3390/ijms23095245>
30. R.A. Friesner, R.B. Murphy, M.P. Repasky, L.L. Frye, J.R. Greenwood, T.A. Halgren, P.C. Sanschagrin and D.T. Mainz, *J. Med. Chem.*, **49**, 6177 (2006); <https://doi.org/10.1021/jm051256o>
31. D. Eisenberg, R. Luthy and J.U. Bowie, *Methods Enzymol.*, **277**, 396 (1997); [https://doi.org/10.1016/S0076-6879\(97\)77022-8](https://doi.org/10.1016/S0076-6879(97)77022-8)
32. C. Colovos and T.O. Yeates, *Protein Sci.*, **2**, 1511 (1993); <https://doi.org/10.1002/pro.5560020916>
33. Structural Analysis, Verification Server; 2011. Available from: <http://nihserver.mbi.ucla.edu/SAVES/>
34. S.C. Lovell, I.W. Davis, W.B. Arendall 3rd, P.I. de Bakker, J.M. Word, M.G. Prisant, J.S. Richardson and D.C. Richardson, *Proteins*, **50**, 437 (2003); <https://doi.org/10.1002/prot.10286>
35. Chem DrawUltra version 8.0.3 for Windows, Cambridge Soft Corporation, a subsidiary of PerkinElmer, Inc. (2014).
36. <https://sourceforge.net/projects/openbabel/files/openbabel/2.4.0/>. License: GNU GPL v2.
37. N.M. O'Boyle, M. Banck, C.A. James, C. Morley, T. Vandermeersch and G.R. Hutchison, *J. Cheminform.*, **3**, 33 (2011); <https://doi.org/10.1186/1758-2946-3-33>
38. E. Harder, W. Damm, J. Maple, C. Wu, M. Reboul, J.Y. Xiang, L. Wang, D. Lupyran, M.K. Dahlgren, J.L. Knight, J.W. Kaus, D.S. Cerutti, G. Krilov, W.L. Jorgensen, R. Abel and R.A. Friesner, *J. Chem. Theory Comput.*, **12**, 281 (2016); <https://doi.org/10.1021/acs.jctc.5b00864>
39. S.G. Franzblau, R.S. Witzig, J.C. McLaughlin, P. Torres, G. Madico, A. Hernandez, M.T. Degnan, M.B. Cook, V.K. Quenzer, R.M. Ferguson and R.H. Gilman, *J. Clin. Microbiol.*, **36**, 362 (1998); <https://doi.org/10.1128/JCM.36.2.362-366.1998>
40. B. Aneja, M. Azam, S. Alam, A. Perwez, R. Maguire, U. Yadava, K. Kavanagh, C.G. Daniliuc, M.M.A. Rizvi, Q.M.R. Haq and M. Abid, *ACS Omega*, **3**, 6912 (2018); <https://doi.org/10.1021/acsomega.8b00582>
41. CLSI, M100 Performance Standards for Antimicrobial Susceptibility Testing, CLSI; Wayne, PA, USA, edn. 29 (2019).
42. A. Bass, E. Abdelhafez, M. El-Zoghbi, M. Mohamed, M. Badr and G.E.D. Abu-Rahma, *J. Adv. Biomed. Pharm. Sci.*, **4**, 81 (2021); <https://doi.org/10.21608/jabps.2020.52641.1113>
43. E.M. Flefel, H.-A. S. Abbas, R.E. Abdel Mageid and W.A. Zaghary, *Molecules*, **21**, 30 (2016); <https://doi.org/10.3390/molecules21010030>
44. B. Sharma, V. Chenthamarakshan, A. Dhurandhar, S. Pereira, J.A. Hendler, J.S. Dordick and P. Das, *Sci. Rep.*, **13**, 4908 (2023); <https://doi.org/10.1038/s41598-023-31169-8>
45. F. Ciriaco, N. Gambacorta, D. Alberga and O. Nicolotti, *J. Chem. Inf. Model.*, **61**, 4868 (2021); <https://doi.org/10.1021/acs.jcim.1c00498>
46. N.M. Raghavendra, D. Pingili, S. Kadasi, A. Mettu and S.V.U.M. Prasad, *Eur. J. Med. Chem.*, **143**, 1277 (2018); <https://doi.org/10.1016/j.ejmech.2017.10.021>
47. M. Jaiteh, A. Zeifman, M. Saarinen, P. Svenningsson, J. Bréa, M.I. Loza and J. Carlsson, *J. Med. Chem.*, **61**, 5269 (2018); <https://doi.org/10.1021/acs.jmedchem.8b00204>
48. S.W. Park, B.H. Lee, S.H. Song and M.K. Kim, *J. Struct. Biol.*, **215**, 107939 (2023); <https://doi.org/10.1016/j.jsb.2023.107939>
49. S.A. Hollingsworth and P.A. Karplus, *Biomol. Concepts*, **1**, 271 (2010); <https://doi.org/10.1515/bmc.2010.022>
50. S. Agnihotry, R.K. Pathak, D.B. Singh, A. Tiwari and I. Hussain, Eds.: D.B. Singh and R.K. Pathak, Protein Structure Prediction. In: Bioinformatics Methods and Applications Academic Press, pp. 177-188 (2022); <https://doi.org/10.1016/B978-0-323-89775-4.00023-7>
51. N.S. Pagadala, K. Syed and J. Tuszynski, *Biophys. Rev.*, **9**, 91 (2017); <https://doi.org/10.1007/s12551-016-0247-1>